Analytical Cellular Pathology 14 (1997) 41–49
IOS Press

DNA measurement of overlapping cell nuclei in thick tissue sections

Liang Ji[a] and James Tucker[b]
[a]*MRC Human Genetics Unit, Crewe Road, Edinburgh, EH4 2XU, UK*
[b]*Edinburgh University Department of Pathology, Teviot Place, Edinburgh EH8 9AG, UK*

Received 7 August 1995
Revised 15 February 1997
Accepted 19 March 1997

Abstract. The paper describes an improved image analysis procedure for measuring the DNA content of cell nuclei in thick sections of liver tissue by absorption densitometry. Whereas previous methods only permitted the analysis of isolated nuclei, the new technique enables both isolated and overlapping nuclei to be measured. A 3D segmentation procedure determines whether each object is an isolated nucleus or a pair of overlapping nuclei; in the latter case the combined optical density is redistributed to the individual nuclei. A selection procedure ensures that only complete nuclei are measured.

The method has been tested on specially-prepared Feulgen-stained 20μ sections of normal liver tissue. The overall distribution of the nuclear DNA measurements shows well-defined diploid and tetraploid peaks, with coefficient of variations of less than 10%. Similar distributions were obtained from both the isolated nuclei and overlapped nuclei sub-populations.

Keywords: Ploidy, DNA content, tissue sections, 3D segmentation, overlaps, image cytometry

1. Introduction

In analytical pathology the measurement of nuclear DNA content, or 'ploidy', has become a major technique for the diagnosis and prognostic evaluation of malignant or pre-malignant specimens, and now shows potential for use in routine pathology. Searching for the relation between nuclear DNA content and cancer prognosis requires accurate DNA measurement. To date this has mostly been carried out by flow cytometry on cell suspensions (either natural body fluids or disaggregated solid tissue specimens), or by image cytometry on cytological preparations (smear, imprints or fine-needle aspirates) [1–3,5,6,9,14,15].

In solid tissue specimens, the correlation between tissue architecture and nuclear DNA content is lost with either of these two techniques. It is therefore only possible to say whether or not aneuploid cells were found in a specimen. The possibility of localising the source of such cells to a particular structural component or region within the specimen could considerably enhance the diagnostic or prognostic potential of such a finding. However, to date no generally applicable method for measuring the DNA content of cell nuclei in solid tissue specimens has been developed.

A previous paper [7] described an absorption densitometry method for measuring the relative DNA content of isolated nuclei in thick tissue sections, the $2^1/_2$D method. The $2^1/_2$D method is based on two facts: firstly, that a thick object can be considered as a series of slices, and the total optical density of the object is given by the sum of the optical density of the individual slices. Secondly, the optical

density of an individual slice as measured by densitometry is relatively unchanged over a substantial range of focal values [7]. Taken together, these facts indicate that, so long as the z projection of an object is within the densitometric focal depth of the optical system, the total absorption for the object can be approximated by measuring its apparent IOD at the central z position.

In this paper we describe a modification to the basic $2^1/_2$D method which enables the DNA measurement of overlapping nuclei to be determined.

2. Materials and methods

2.1. Overview

The analysis process consists of five steps. Firstly, Feulgen-stained thick tissue sections are prepared and mounted by a method designed to minimise optical aberrations. Secondly, a sequence of section images with equal z distance is digitised. Thirdly, a three-dimensional segmentation procedure is used to localise individual nuclei. A selection procedure is then used eliminate any incomplete nuclei. Lastly, the integrated optical density (IOD) values of the remaining nuclei are measured.

2.2. Three-dimensional segmentation and densitometric measurement

The segmentation procedure has three purposes: (i) to find isolated nuclei; (ii) to separate touching or overlapping nuclei; and (iii) to provide an appropriate modification of pixel density values in overlapped nuclei. The desired output from the segmentation process is a candidate list of segmented nuclei (each nucleus with its 2D shape and pixel densities, and z position of the image of the nucleus which has the highest contrast value).

The 3D segmentation procedure uses a combination of a series of 2D gradient images and density analysis. The process is based on the assumption that, since the nuclei are approximately spherical or ovoid, two overlapping nuclei are either circular/elliptical in x–y outline but far apart in the z direction (complete overlaps), or the resulting object boundary must show indentations and can therefore be detected by shape analysis (partial overlaps).

The 2D gradient is defined by the maximum of the gradient in either the horizontal (x) or vertical (y) direction. Both x and y gradients are calculated by convolution with a $(1\ 0\ -1)$ or $(-1\ 0\ 1)$ mask on a smoothed image. The vertical gradient is obtained from a horizontally-smoothed image (using a $(1\ 2\ 1)$ smoothing filter in the x direction); correspondingly, the horizontal gradient is obtained from a vertically smoothed image. The resulting gradient image of each section is thresholded at a fixed level and then labelled to obtain individual connected components. The outermost boundary of each component is used to define the region of interest and then to recreate the original nucleus. This can avoid complications caused by holes. The resulting objects are smoothed using opening [10,11] to remove noise and branches (incomplete edge elements), and their centre coordinates added to a candidate object list.

Initially the candidate list is the copy of the result from the segmentation of the first section. The resulting objects from the rest of the sections are then compared in turn with the objects in the candidate list. A new object is added to the list if it does not overlap with any candidate. If overlapping occurs the mean gradients are compared and the one with the lowest mean gradient value is deleted from the candidate list unless their z positions are far apart. The nucleus with the higher IOD is added to the list (or retained if already there).

A shape analysis is carried out on every object on the candidate list. Further analysis is carried out only on elliptical objects. The shape analysis is based on the comparison between the object and its convex hull, and between the longest chord and the shortest chord which are obtained from the minimum rectangle which can contain the object. All elliptical candidates are then compared to each other to decide whether the object represents a pair of overlapping nuclei; if so then the densities of both nuclei need to be modified as described below.

The IOD for each isolated nucleus is calculated as the sum of the individual pixel ODs within the segmented object area, corrected by a skirt value [12] to compensate for the background. The skirt value for a segmented object is calculated from the difference between two dilated objects, the larger obtained by Euclidean dilation of the corresponding nucleus by a radius 4 disc, and the smaller one by a disc of radius 2. The average OD of the lowest 70% of these pixels is used as the background value.

The same method is applicable to complete overlaps where the skirt compensates for the density contribution of the out-of-focus nucleus. However for partially overlapping nuclei the pixel density ODs must be modified after 3D segmentation. The method used to modify the optical density values when a partial overlap is detected is shown diagrammatically in Fig. 1.

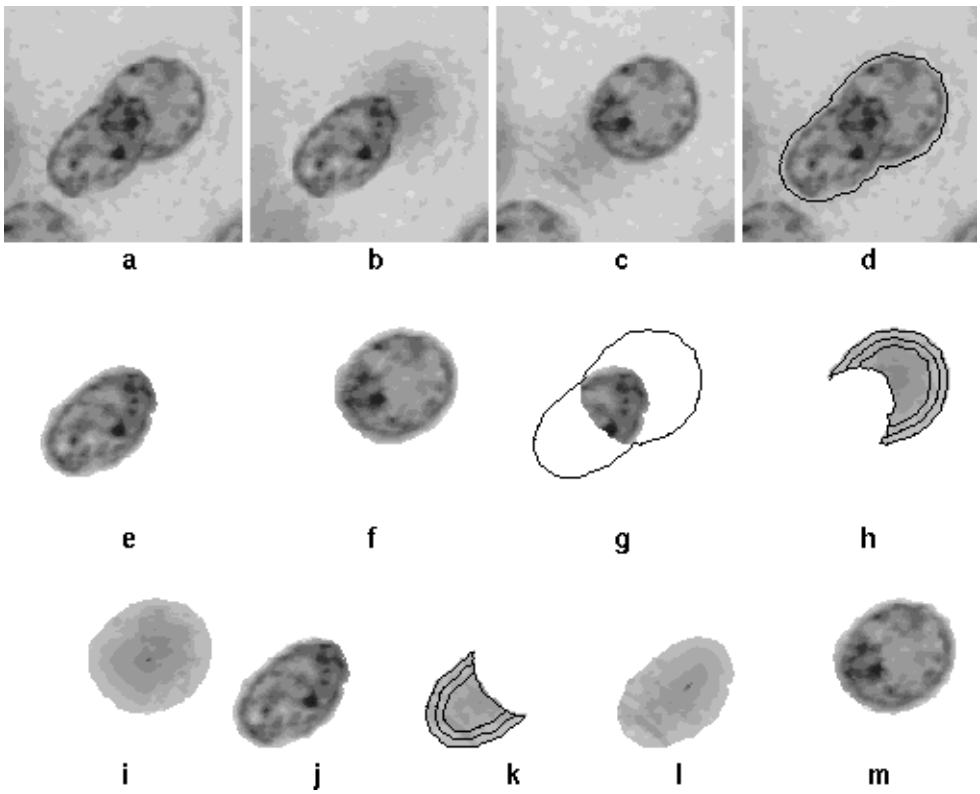

Fig. 1. Modifying density values in partial overlaps. (a) Compound image; (b), (c) two infocus sections for nuclei A, B chosen by the gradient method; (d) the region of interest, i.e., the union of the two nuclei; (e), (f) segmentation of the two nuclei in different focal planes; (g) intersection region of the two nuclei in which modification of the grey values is needed; (h), (i) reconstruction of the defocussed nucleus B; (j) cell A with OD component values from cell B in overlap region subtracted; (k), (l), (m) repeat of this process on cell B.

The compound image is formed by the highest optical density value of each pixel column in all sections. Figure 1a clearly shows the overlap region in which the pixel OD modification is needed. The appropriate density contribution for each defocused nucleus image is obtained by assuming that the grey values are approximately the same in each shell (Fig. 1h, k). These values are subtracted from the in-focus image pixel values for each nucleus. Finally, a background skirt density, calculated as above, is subtracted from every pixel in each segmented nucleus.

Because the diameter of a typical liver cell nucleus is 8–12μ, and the thickness of the slide is 15–20μ, a substantial proportion of the objects in the tissue section images correspond to partial nuclei which are cut by the top or bottom boundaries of the tissue section. An automatic object selection procedure is therefore used to eliminate measurements from incomplete nuclei. Full details of the object selection procedure are given in [7].

2.3. Experimental measurement procedure

The verification experiments were performed on 20μ sections of human liver tissue blocks. The blocks were formalin fixed and paraffin embedded. The sections were stained by the Feulgen method, cleared in methyl benzoate and mounted using Cover Bond with glass cover slips. Full details of the procedure are given in [7].

Fields were chosen arbitrarily in the tissue sections, except that fields containing large numbers of pyknotic cells were excluded. The selected fields were digitised on a Zeiss AxioHOME computerised microscope [4] using a 100 NA 1.3 oil immersion objective at a resolution of 10 pixels/μ. This microscope was modified by adding a Sony skeleton linear encoder to the focus (z) axis with a readout LH20 display (0.5μ resolution). For each field 32 images were grabbed at different z positions separated by 1.0μ. The centre z position was chosen to correspond approximately to the centre position of the tissue section at each field position.

A total of 155 fields were digitised, and the data were transferred to a Sun Sparc10 workstation for further analysis. The intensity values of each pixel were transformed to optical density (OD) values prior to analysis. This OD transformation was carried out by table look up, using a calibration table obtained by measurements on a photographic test slide which had previously been measured on a microdensitometer [7,12].

3. Results

Figure 2 shows an example of sections of a typical pair of nuclei which are completely overlapped (only 24 middle sections are shown). Figure 2a shows the optical density and Fig. 2b shows the gradient image. No matter which section is chosen and what thresholding level is used, the result from thresholding the optical density image Fig. 2a is always a single object. However, if thresholding is carried out on the gradient images (Fig. 2b), two objects separated in the z direction are obtained.

Figure 3 shows an example of a partial overlap, in which the in-focus sections of the two nuclei are close to each other, so that only one gradient-image object is obtained. However, the boundary indentation in the in-focus object can be clearly seen.

In a visual inspection of the 155 fields analysed, a total of 2340 nuclei were detected, of which 1401 were considered to be complete. The automatic system selected a total of 1274 complete nuclei, of which 631 were classified as isolated, 643 as overlaps.

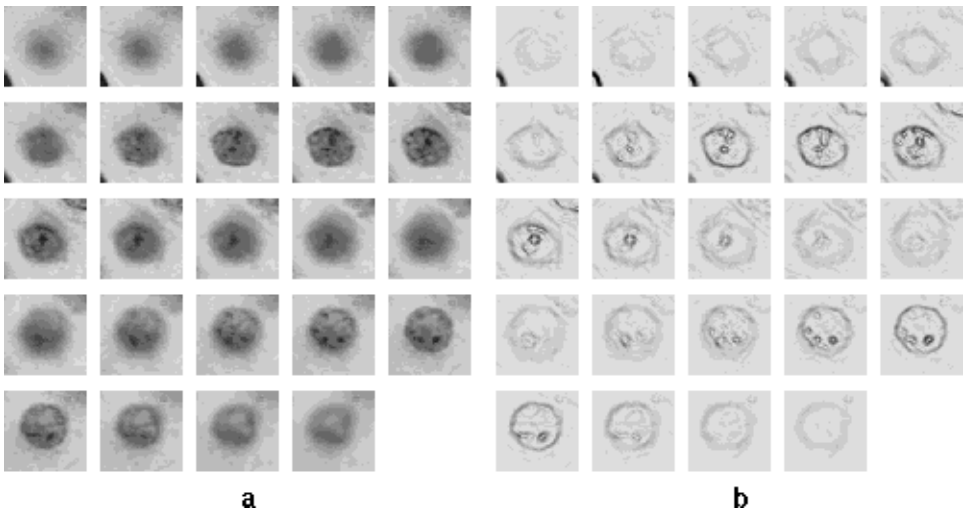

Fig. 2. Sequential z-section images of a complete overlap between two nuclei. (a) Intensity images, (b) gradient images. Size – x, y 11μ; z interval 1μ.

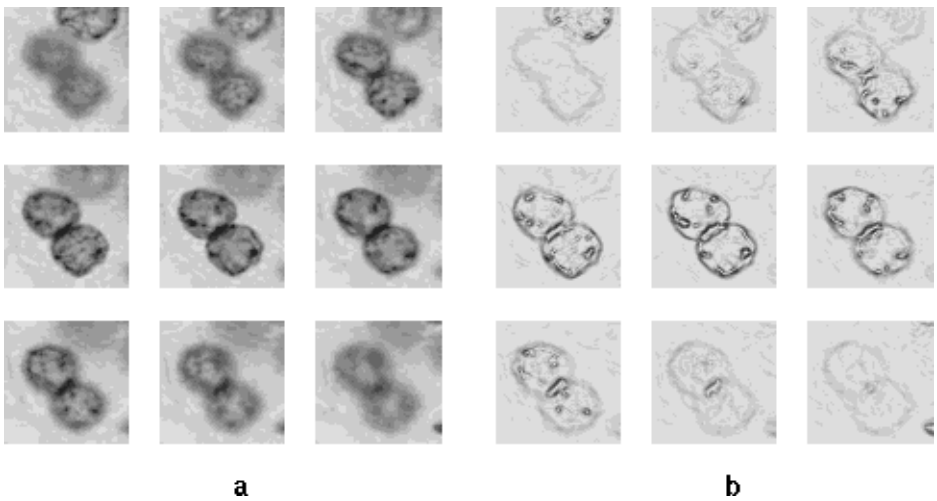

Fig. 3. Sequential z-section images of a partially overlap between two nuclei. (a) Intensity images, (b) gradient images. Size – x, y 13μ; z interval 1μ.

The overall histogram of the DNA measurements for all nuclei is shown in Fig. 4. The histogram clearly shows distinct peaks corresponding to the diploid (2C) and tetraploid (4C) cell populations. Table 1 shows the statistical characteristics for the peaks, and the relationship between their means.

To investigate the measurement accuracy of the method for analysing overlapped cell nuclei, the histograms of the IOD values of the 643 overlapped nuclei was compared both visually and analytically with that of the 631 isolated nuclei. These are shown in Figs 5a and 5b.

The statistical analysis of the two histograms was carried out by fitting a Gaussian distribution to the 2C and 4C peaks, estimating the number of nuclei in each peak, and then computing the remainders in the $<$2C, S phase, and $>$4C regions by the rectangle method [13]. The results are also shown in Table 1.

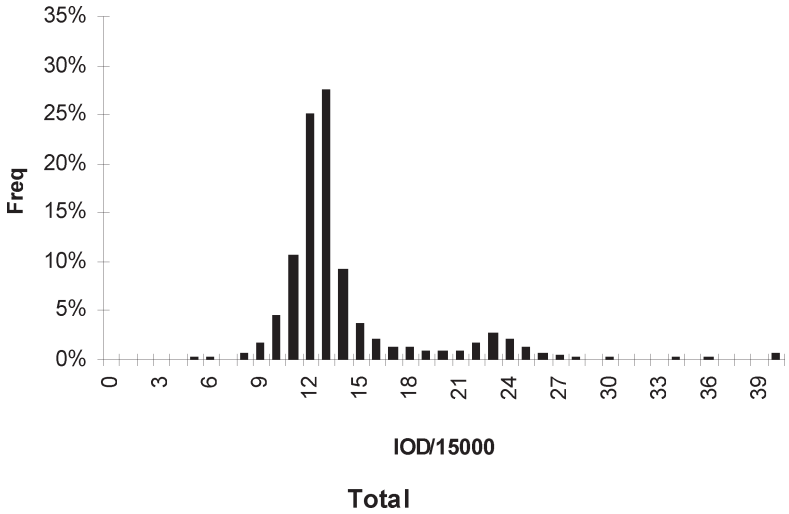

Fig. 4. Histogram of IOD values for all selected cell nuclei.

Table 1
Summary statistics of ploidy distributions

	Totals	Singles	Overlaps
<2C Count	45	38	41
% Count (<2C)	4%	6%	6%
2C Count	994	471	457
% Count (2C)	78%	75%	71%
2C Mean	178,644	181,783	176,580
2C c.v.	9.51%	6.10%	9.12%
S-phase count	106	41	86
% Count (S)	8%	7%	13%
4C Count	96	69	40
% Count (2C)	8%	11%	6%
4C Mean	346,462	347,045	342,843
4C c.v.	4.38%	5.57%	4.58%
>4C Count	28	6	14
% Count (>4C)	2%	1%	2%
Total count	1274	631	643
4C/2C Mean	1.94	1.91	1.94

4. Discussion

The method described provides a new and improved way of measuring the DNA content of cell nuclei in thick sections of liver tissue. Whereas the previous $2^1/_2$D method only permitted the analysis of isolated nuclei, the new technique enabled both isolated and overlapping nuclei to be measured. This provides a far greater number of nuclei which are suitable for analysis in each field.

The histogram for the cell nucleus DNA measurement provides evidence that the method gives accurate results. The histogram clearly shows distinct peaks corresponding to the diploid (2C)

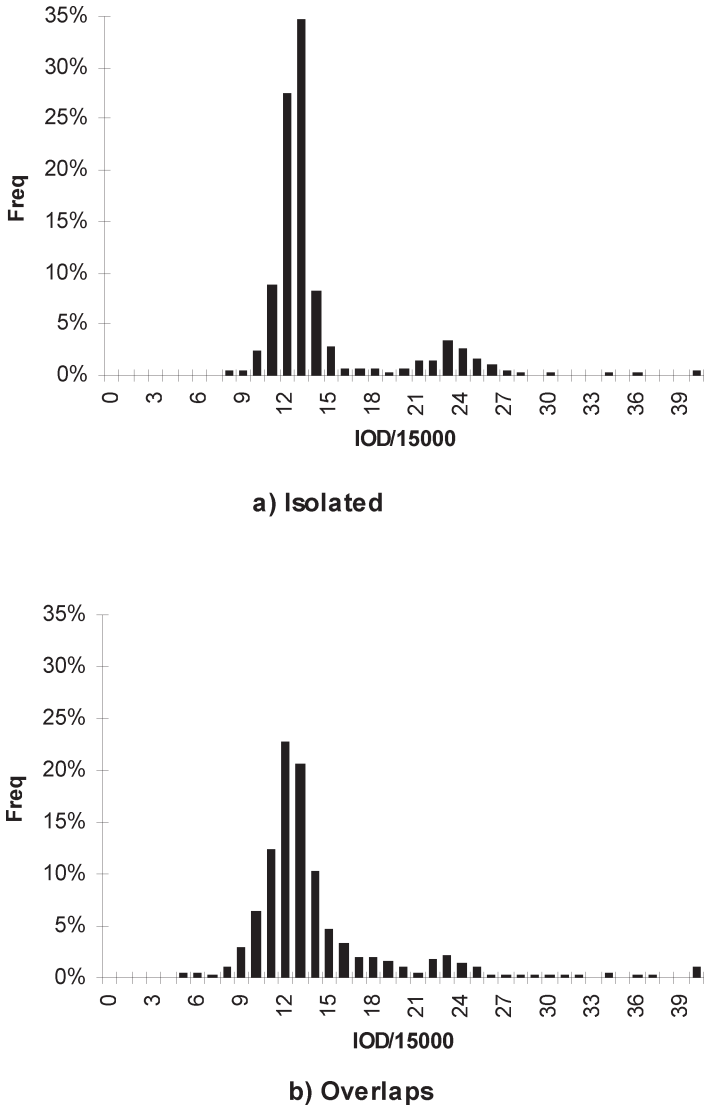

Fig. 5. (a) Histograms of isolated cells from automatic 3D segmentation. (b) Histograms of overlapping cells from automatic 3D segmentation.

and tetraploid (4C) cell populations, and these show a low coefficient of variation (Table 1) compared with other methods such as confocal microscopy [8]. Also, the mean values corresponding to these peaks show a ratio close to the value of 2 expected from the biological model.

Further evidence of the accuracy of the measurements is provided by the similarity between the characteristics of the histograms for overlapped and isolated nuclei (Fig. 5 and Table 1). The only major difference between the two populations is seen in the relatively higher 'S-phase' region count and lower '4C' region count in the overlap population. This can be accounted for by occasional errors in the pixel optical density modification process; and by the inclusion of a few overlaps with partially sectioned nuclei.

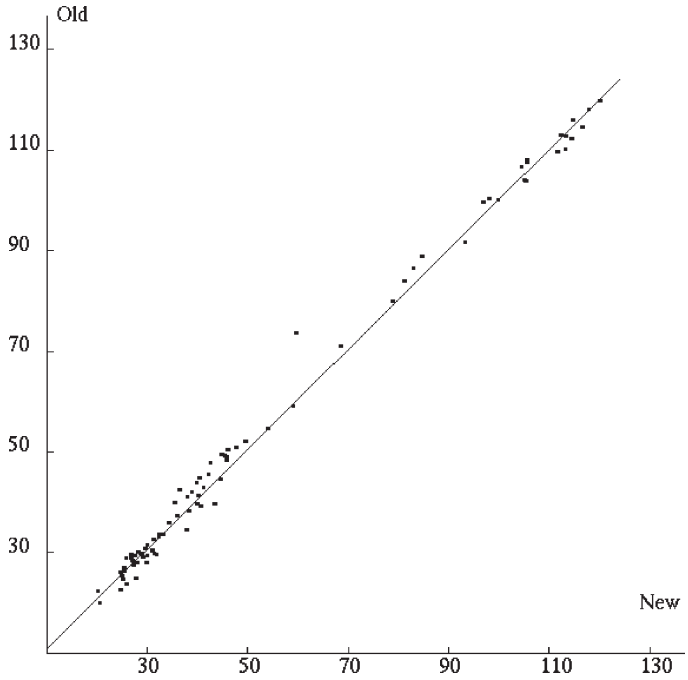

Fig. 6. Comparison of DNA measurements on isolated nuclei using the old ($2^1/_2$D) and new 3D segmentation methods.

The improved $2^1/_2$D procedure uses the gradient images from each individual section for 3D segmentation instead of just one compound image as in the previous method [7]. This allows a much larger proportion of the nuclei contained in the 20μ liver tissue sections to be measured than in the previous results because overlapping nuclei, as well as isolated nuclei, can now be measured. The tests carried out indicate that most (approximately 90%) of the complete nuclei can now be measured.In the case of isolated nuclei, the two methods give very similar results. Figure 6 shows the scatter diagram of the IOD measurement on the same isolated nuclei using the two different segmentation methods and the linear regression line.

One noticeable difference between the two methods is the somewhat lower proliferation index (proportion of tetraploid nuclei) obtained in these experiments compared with the earlier report. This is caused by the fact that pairs of heavily overlapping nuclei were not detected by the earlier compound-image method of analysis, but are measured as a single high-ploidy nucleus. This segmentation error is eliminated in the new method.

A disadvantage of the new method is the increased time needed to process each 32-section field image (approximately 2 mins/field on the Sun Sparc10 workstation) compared with the previous method (1 min/field). The increased time is incurred by the need to carry out several algebraic manipulations on each optical section image, compared with the segmentation on a single compound image in the previous method. Neverthless, the method is much quicker than deconvolution procedures carried out on the image sections (results not shown).

A limitation of the method is that, in its present form, it is only satisfactory for analysing overlap images involving two relatively simple nuclei. Further extensions to the current methods are required to enable nuclear DNA content to be measured in more complex solid tissue samples than the relatively simple liver tissue measured here.

5. Conclusion

A method for measuring the DNA content of both isolated and overlapped cell nuclei in thick liver tissue sections by computerised absorption densitometry has been devised and investigated. The measurements show that good accuracy is obtained for isolated, partially overlapped and completely overlapped nuclei. The method therefore provides a useful step in the quest to find more general methods of measuring total DNA content of cell nuclei in solid tissue.

Acknowledgements

We wish to thank Mr. D. Bishop of the Edinburgh University Pathology Department for preparing specimens for this work.

References

[1] T.W. Bauer, R.R. Tubbs, M.G. Edinger, G.N. Suit Gephardt and H.S. Levin, A prospective comparison of DNA quantitation by image and flow cytometry, *Am. J. Clin. Pathol.* **93** (1990), 322–326.
[2] A. Berner, H.E. Aanielsen, N.O. Juul, M.E.H. Juul, E.O. Pettersen, A. Reith, J.M. Nesland and S.D. Foss, Caveats in the estimation of DNA-ploidy in paraffin embedded specimens of primary prostate cancer and lymph node metastases by flow and image cytometry, *Anal. Cell Pathol.* **5** (1993), 339–352.
[3] S. Bosari, B.D. Wiley, W.M. Hamilton, J.M. Dugan, L.B. Cook and A.K.C. Lee, DNA measurement by image analysis of paraffin-embedded breast carcinoma tissue: A comparative investigation, *Am. J. Clin. Pathol.* **96** (1991), 698–703.
[4] G. Brugal, R. Dey, B. Krieff, J.M. Chassery, H. Tanke and J.H. Tucker, HOME – Highly Optimized Microscope Environment, *Cytometry* **13** (1992), 109–116.
[5] C. Cope, L. Delbridge, J. Philips and M. Friedlander, Comparison of image analysis and flow cytometric determination of cellular DNA content, *J. Clin. Pathol.* **44** (1991), 147–151.
[6] R.E. Fausel, W. Burleigh and D.B. Kaminsky, DNA quantification in colorectal carcinoma using flow and image analysis cytometry, *Anal. Quant. Cytol. Histol.* **30** (1990), 21–27.
[7] L. Ji, J. Lauder and J. Tucker, Nuclear DNA quantitation in thick tissue sections by absorption densitometry, *AQCH*, 1995 (in press).
[8] J.P. Rigaut, J. Vassy, P. Herlin, F. Duigou, E. Masson, D. Briane, J. Foucrier, S. Carvajal-Gonzalez, A.M. Downs and A.-M. Mandard, Three-dimensional DNA image cytometry by confocal scanning laser microscopy in thick tissue blocks, *Cytometry* **12** (1991), 511–524.
[9] E.K.W. Schulte, Standardization of the Feulgen reaction for absorption DNA image cytometry: a review, *Anal. Cell Pathol.* **3** (1991), 167–182.
[10] J. Serra, *Image Analysis and Mathematical Morphology*, Academic Press, London, 1982.
[11] J. Serra, Introduction to mathematical morphology, *Comp. Graphics Image Proc.* **35** (1986), 283–305.
[12] J.H. Tucker, O.A.N. Husain, K. Watts, S. Farrow, R. Bayley and M.H. Stark, Automated densitometry of cell populations in a continuous motion imaging cell scanner, *Applied Optics* **16** (1987), 3315–3324.
[13] M.A. Van Dilla, P.N. Dean, O.D. Laerum and M.R. Melamed, *Flow Cytometry: Instrumentation and Data Analysis*, Academic Press, London, 1985.
[14] G. Willin, U. Askensten, M. Backdahl, L. Grimelius, G. Lundell and G. Auer, Cytochemical assessments of the nuclear DNA distribution pattern by means of image and flow cytometry in thyroid neoplasms and non-neoplastic thyroid lesions. A comparative methodological study, *Acta Chir. Scand.* **155** (1989), 251–258.
[15] T. Yamamoto, H. Horiguchi, H. Kamma, M. Noro, T. Ogata, Y. Inage, E. Akaogi, K. Mitsui, M. Hori and M. Isobe, Comparative DNA analysis by image cytometry and flow cytometry in non-small cell lung cancer, *Japanese Journal of Cancer Research* **85** (1994), 1171–1177.